

RESEARCH

Open Access



# Environmental change increases the transmission risk of visceral leishmaniasis in central China around the Taihang mountains

Ze Meng<sup>1,3†</sup>, Pei-Wei Fan<sup>2,4†</sup>, Zi-Xuan Fan<sup>2†</sup>, Shuai Chen<sup>2</sup>, Hou Jiang<sup>2,4</sup>, Yue Shi<sup>5</sup>, Ling Yao<sup>2,4</sup>, Jian-Yi Yao<sup>5</sup>, Ye-Ping Wang<sup>5</sup>, Meng-Meng Hao<sup>2,4</sup>, Wen-Qi Xie<sup>2,4</sup>, Yong-Qing Bai<sup>6</sup>, Qian Wang<sup>7,8</sup>, Kai Sun<sup>9</sup>, Xiao-Lan Xie<sup>10</sup>, Jian-Wei Zhou<sup>11</sup>, Dong Jiang<sup>2,4</sup>, Can-Jun Zheng<sup>5\*</sup>, Hua Wu<sup>1,12,3\*</sup>, Tian Ma<sup>13,14\*</sup> and Fang-Yu Ding<sup>2,4\*</sup>

## Abstract

**Background** Visceral leishmaniasis is a neglected life-threatening sandfly-borne disease, which brings a growing public health threat in Central China around the Taihang Mountains. However, the spatiotemporal dynamics of visceral leishmaniasis in the local community and the potential driving factors remain poorly understood.

**Methods** We analyzed the spatiotemporal patterns of new reported visceral leishmaniasis cases in the region from 2006 to 2023, and combined random forest modeling approach with environmental covariates to identify the main influencing factors related to transmission risk of the disease.

**Results** Our results show that there was a total number of 800 reported human visceral leishmaniasis cases, affecting 29 cities, and 113 counties across the region, exhibiting a geographic expansion of the disease during this period, especially in Shanxi province. Two high-risk clusters were identified in the study. Environmental change-related factors, including standardized precipitation deviation, forest cumulative change ratio, and normalized difference vegetation index (NDVI) cumulative change, played important roles in increasing the transmission risk of visceral leishmaniasis, with their relative contributions summing up to 66.17%.

## Background

Visceral leishmaniasis (VL), also known as kala-azar, is a vector-borne disease caused by intracellular protozoa from the genus *Leishmania* [1, 2]. The parasite is typically transmitted through the bite of an infected female sandfly [3]. *Leishmania* requires a host to ensure its survival, typically an animal such as dogs or rodents (common reservoirs), while humans act as accidental hosts [4, 5]. In symptomatic infections, the most common signs and clinical manifestations include prolonged fever, weakness, night sweats, anorexia, weight loss, pallor, lymphadenopathy, hepatomegaly, and splenomegaly [6, 7]. If

<sup>†</sup>Ze Meng, Pei-Wei Fan and Zi-Xuan Fan contributed equally to this work.

\*Correspondence:  
Can-Jun Zheng  
zhengcj@chinacdc.cn  
Hua Wu  
xzwhua@163.com  
Tian Ma  
tian.ma@yale.edu  
Fang-Yu Ding  
dingfy@igsrr.ac.cn

Full list of author information is available at the end of the article



© The Author(s) 2025. **Open Access** This article is licensed under a Creative Commons Attribution-NonCommercial-NoDerivatives 4.0 International License, which permits any non-commercial use, sharing, distribution and reproduction in any medium or format, as long as you give appropriate credit to the original author(s) and the source, provide a link to the Creative Commons licence, and indicate if you modified the licensed material. You do not have permission under this licence to share adapted material derived from this article or parts of it. The images or other third party material in this article are included in the article's Creative Commons licence, unless indicated otherwise in a credit line to the material. If material is not included in the article's Creative Commons licence and your intended use is not permitted by statutory regulation or exceeds the permitted use, you will need to obtain permission directly from the copyright holder. To view a copy of this licence, visit <http://creativecommons.org/licenses/by-nc-nd/4.0/>.

**Conclusions** Our findings provide a better understanding of the spatiotemporal dynamics and driving factors of visceral leishmaniasis recurrence across Central China around the Taihang Mountains, which underscore prevention and control measures should be taken immediately to reduce the risk.

**Keywords** Visceral leishmaniasis, Spatiotemporal dynamics, Environmental change, Transmission risk

left untreated, VL may cause multisystem disease, and result in secondary infections and death [7, 8]. Among parasitic diseases, VL has the second-highest mortality rate, surpassed only by malaria [9, 10]. In addition, it is widespread across all continents except Oceania, with approximately 500,000 new cases reported annually [2, 9, 11].

In China, previous studies suggest that the earliest cases of VL appeared in the 1880s [12, 13], while the first parasitologically confirmed case of VL in China was reported in 1904, involving a German soldier [13–15]. Following this, more cases were reported across various regions, including the provinces of Jiangsu, Shandong, Hebei, Hunan, Shanxi, Shaanxi, Gansu, Xinjiang, Sichuan, Jiangxi, and Liaoning [13, 14, 16, 17]. After the establishment of the People's Republic of China in 1949, widespread interventions such as diagnosis and chemotherapy of patients, identification, isolation, and disposal of infected dogs, and residual insecticide indoor spraying for vector control were implemented to control VL, leading to a gradual decline in cases [1]. For example, there were approximately 530,000 cases of VL in 1951, and the disease had nearly disappeared from the plains north of the Yangtze River by 1958 [18, 19]. However, by the late 1980s, the implementation of the “Western Development Strategy” created favorable habitats for the transmission of VL, leading to a resurgence and outbreak of the disease in western and central China [20]. Between 2004 and 2016, the majority of cases were reported in Xinjiang, Gansu, and Sichuan, accounting for more than 90% of all cases reported nationwide [21, 22].

In recent years, there has been an upward trend in VL cases in Central China [23, 24], posing a growing public health threat around the Taihang Mountains. However, the spatiotemporal dynamics of VL in the local community and the potential driving factors remain poorly understood. To address this gap, we conducted a spatiotemporal analysis of VL cases reported between 2006 and 2023, aiming to identify underlying drivers and offer new insights for disease prevention and control.

## Materials and methods

### Study area

The study area is geographically situated between latitudes 32°N and 42°N, and longitudes 112°E and 118°E, encompassing four major regions surrounding the Taihang Mountain Range: Beijing, Hebei, Shanxi, and Henan (Fig. 1). The Taihang Mountains extend in a

north-northeast to south-southwest direction, serving as a natural divider between the North China Plain to the east and the Loess Plateau to the west. The terrain varies significantly, with elevations ranging from −4 to 2,919 m and an average elevation of 636.28 m. The annual mean temperature ranges from 10.64 °C to 12.16 °C, while annual precipitation varies from 326.74 to 885.76 mm [25]. Socioeconomically, all four regions (Beijing, Hebei, Shanxi, and Henan) had Gross Domestic Product exceeding 2.5 trillion Chinese Yuan (CNY) in 2023 [26–29].

### Human VL cases

In this study, human VL case data from 2006 to 2023 were obtained from the Chinese Center for Disease Control and Prevention (China CDC) and analyzed. A total of 800 cases were confirmed through clinical diagnosis and laboratory testing, while suspected VL cases were excluded from this study due to their inherent uncertainty.

### Terrain factor

The sandfly, the primary vector of VL, is widely distributed in mountainous regions [30, 31], and previous study has shown that topography is a significant factor influencing sandfly distribution [32]. In this study, elevation was chosen as a topographical variable that may affect the presence of VL [23]. Elevation data with a spatial resolution of 90 m were obtained from the Consultative Group on International Agricultural Research Consortium for Spatial Information [33]. The elevation dataset was then processed and aggregated from the grid level to the county level using ArcGIS 10.8.

### Environmental factors

Climate change influences vector-borne diseases in multiple ways, with numerous studies demonstrating the significant impact of climatic variables on parasitic and zoonotic diseases [34, 35]. For example, temperature affects the development, reproduction, and lifespan of sandflies [36, 37], while precipitation influences the distribution and abundance of sandfly populations [37, 38]. Moreover, changes in temperature condition and precipitation pattern may alter breeding sites, which are essential for the survival and proliferation of sandflies [39, 40]. The climate data utilized in this study include surface precipitation rates and 2-meter mean air temperatures, which were available from the ERA-5 reanalysis of historical observations at a daily temporal resolution on a regular 0.25° × 0.25° grid [25]. Based on these datasets, we

generated annual mean temperature and annual precipitation for the years 1970 to 2023. Then we used data from 1970 to 2005 as the baseline to calculate the standardized temperature deviation and the standardized precipitation deviation for 2006 to 2023. The detailed information about generating long-term climate change index can be found elsewhere [41, 42].

Ecological environments have a significant impact on vector-borne diseases, with changes in land cover types notably affecting VL [43–45]. On one hand, the abundance of sandflies varies across different land cover types, with some studies indicating higher infection rates in forested areas [46, 47]. On the other hand, the expansion of human activity areas increases exposure risks, contributing to a higher risk of VL [46]. We used the Annual International Geosphere-Biosphere Programme (IGBP) classification from the MCD12Q1 Version 6 data product for reclassification. Using 2005 land cover data as a baseline, we calculated the cumulative change in the proportions of forest, cropland, and urban areas for each county to explore the long-term impact of land cover type changes on the number of VL cases [48]. Additionally, some studies have shown that the Normalized Difference Vegetation Index (NDVI) is a key factor influencing sandfly distribution [49, 50]. Therefore, we used NDVI data from the MOD13A1 Version 6.1 product, with a spatial resolution of 500 m and 16-day intervals. We synthesized the maximum NDVI values for each year and extracted them at the county level. Similarly, using 2005 as the baseline, we calculated NDVI cumulative change over time to assess the long-term impact of vegetation changes on the number of VL cases [51].

#### Socioeconomic factors

Previous studies have shown the relevance of socioeconomic factors to the transmission of VL [9, 52–54]. For VL, low-income people show a greater susceptibility, which may be due to poor sanitation and inadequate nutrition [9, 54]. Additionally, some studies have found that population size is associated with the transmission of VL [24, 55]. We used population distribution data with a spatial resolution of 1 km from the LandScan database (<https://landscan.ornl.gov/>) to calculate the annual population for each county. To reduce data skewness, we applied a logarithmic transformation to the population data. Gross Domestic Product (GDP) data were sourced from Scientific Data [56].

#### Space-time cluster approach

Space-time cluster analysis was conducted using SaTScan 10.2.4 (64-bit version) to identify high-risk and low-risk clusters of VL cases. The maximum spatial cluster size was set at 50% of the population. To enhance the statistical power of our analysis, we performed 999 standard

Monte Carlo simulations. Clusters with a  $p$ -value of less than 0.05 were considered statistically significant in our study.

#### Random forest

The models were developed and evaluated using the 64-bit R version 4.4.1. In the R statistical programming environment, we utilized the randomForest and caret packages for analysis. The randomForest package was used to build the random forest model, while the caret package was used for model training and evaluation, including cross-validation.

In the present study, we calculated the annual total number of VL cases for each county using unique county codes and spatially matched these data with relevant driving factors. Data processing was conducted using Python version 3.8. To model the relationship between VL cases and various environmental and demographic factors, we first divided the dataset into records with cases (cases > 0) and those without cases (cases = 0). Since the number of non-case records was significantly higher, we randomly sampled an equal number of non-case records to balance the dataset. This process was repeated 50 times to capture potential variability in the random sampling. In each iteration, the balanced dataset was shuffled. We used the balanced data to build the random forest model and applied 5-fold cross-validation using the caret package. The cross-validation was stratified by the year of case occurrence to ensure temporal consistency across the folds.

## Results

#### Spatiotemporal distribution of VL cases

We mapped the spatiotemporal distribution of clinically and laboratory-confirmed VL cases at the county level from 2006 to 2023 in the four regions near the Taihang Mountains (Fig. 2). The earliest case of VL was reported in March 2006 in western Shanxi province. In 2007, three cases were reported across two counties in Henan province. In 2008 and 2009, Shanxi reported one case each year, while two cases were reported there in 2010. Between 2011 and 2014, the total number of cases reported annually across the four major regions did not exceed 10, with 5, 2, 7, and 5 cases, respectively. During this period, Beijing reported its first case in 2013, followed by Hebei province in 2014. Since 2015, the number of cases has gradually increased, and by 2020, the total number of cases reported across the four regions exceeded 100 for the first time. Overall, during the period from 2006 to 2023, Shanxi province has consistently accounted for the majority of the total cases among the four regions (586 cases), followed by Henan (129 cases), Hebei (71 cases), and Beijing (14 cases). These cases are predominantly concentrated in the central and western

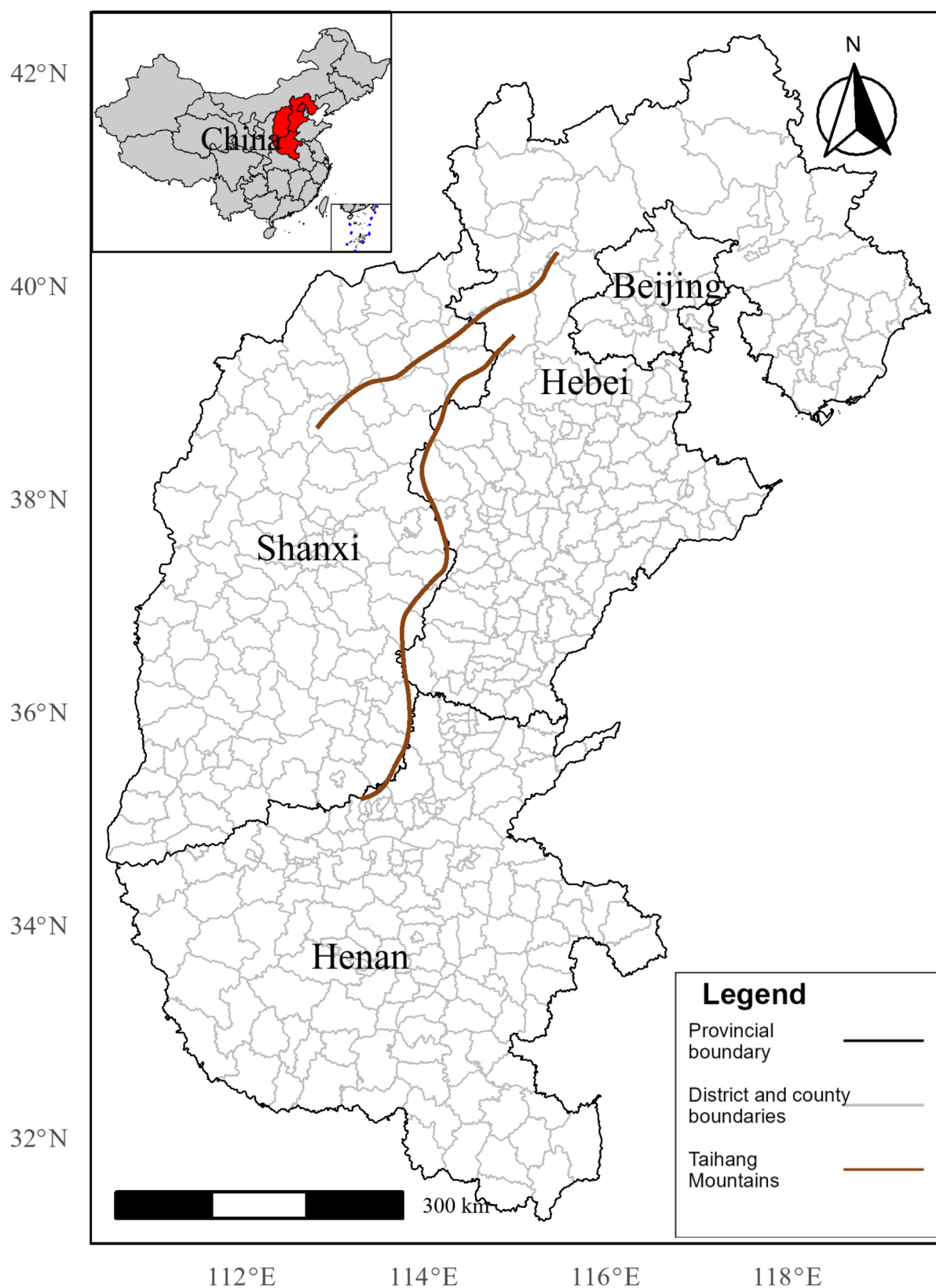


**Fig. 1** Study Area: Regions Surrounding the Taihang Mountains. The study area encompasses Beijing (16 districts, covering 16,000 square kilometers with a population of 22 million), Hebei province (11 cities, 167 districts, covering 188,800 square kilometers with a population of 74 million), Shanxi province (11 cities, 117 districts, covering 156,700 square kilometers with a population of 35 million), and Henan province (17 cities, 136 districts, covering 167,000 square kilometers with a population of 98 million)



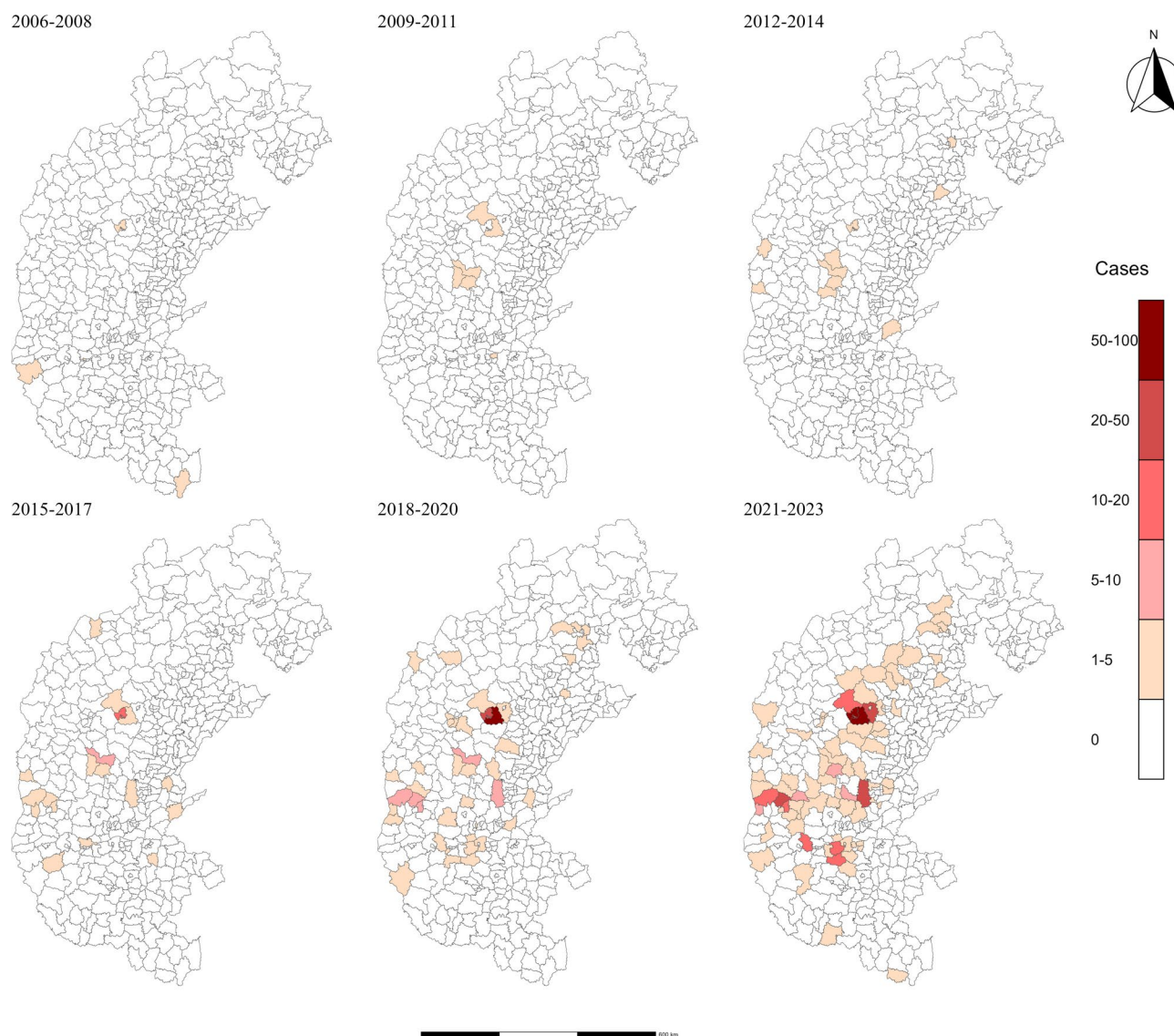


**Fig. 2** Spatial Distribution of VL Cases from 2006 to 2023

areas of these regions, and both the geographic range and number of VL cases have expanded over time (Figs. 2 and 3).

The monthly variation of VL cases across the four regions was also analyzed. Although there has been a significant increase in cases each year, no specific seasonal or monthly patterns have been observed (Fig. 3).

#### Space-time clustering analysis

The spatiotemporal scanning analysis identified two significant high-risk clusters of VL cases. The first main cluster was located in Pingding county, Yangquan city in the eastern part of Shanxi province, with coordinates at 37.84 N and 113.75 E, covering a radius of 55.21 km, for the period from 2017 to 2023. This cluster included 16 districts and counties in the eastern region of Shanxi

province and the western region of Hebei province. During the study period, this area reported 395 cases against an expected count of 3.24, demonstrating significant spatiotemporal aggregation with a relative risk (RR) of 239.59. The log-likelihood ratio (LLR) was 1622.84 ( $P < 0.001$ ). Another notable high-risk cluster was located in Yuanqu county, Yuncheng city in the southern part of Shanxi province, centered at coordinates 35.21 N and 111.81 E, with a larger radius of 211.75 km, for the period from 2020 to 2023. This cluster encompassed a broader area, including 130 districts and counties in the southern part of Shanxi province and the northeastern part of Henan province, with a total of 239 observed cases compared to an expected 39.95. The RR for this cluster was 8.10, with an LLR of 257.17, demonstrating significant spatiotemporal aggregation ( $P < 0.01$ ) (Fig. 4; Table 1).



**Fig. 3** Monthly Variation of VL Cases across four regions from 2006 to 2023

Additionally, three low-risk clusters were also identified, with specific details provided in the Supplementary Materials (Figure S1 and Table S1).

#### Driving factors of VL recurrence

The performance of the random forest model was evaluated through a process of repeated random sampling, where 50 iterations were conducted to create a balanced dataset by combining cases with non-cases, followed by training the model and assessing its predictive accuracy. The average correlation coefficient ( $R$ ) from five-fold cross-validation was 0.577, indicating that the model demonstrated applicability in capturing the relationship between the predicted and observed values. The random forest model was employed to assess the influence of various environmental and demographic factors on VL cases. The normalized importance of each variable was calculated as a percentage, reflecting the relative contributions

of each factor to the model's predictive performance. Among the variables, standardized precipitation deviation emerges as the most significant predictor, accounting for 17.95% of the total explained variation. This is followed by elevation (14.22%), forest cumulative change ratio (12.29%), NDVI cumulative change (11.15%), and the log of population (11.00%). Standardized temperature deviation (9.43%) and GDP (8.61%) also contribute notably, whereas urban cumulative change ratio (7.82%) and crop cumulative change ratio (7.54%) have the lowest contributions. Despite this, they still play meaningful roles in the overall model. In addition, the results further underscore the dominant role of environmental factors, which collectively account for 66.17% of the total explained variation. This is followed by socioeconomic factors (19.61%) and terrain factors (14.22%) (Table 2).

The increase in the standardized deviations of precipitation and temperature has contributed to the rise in VL

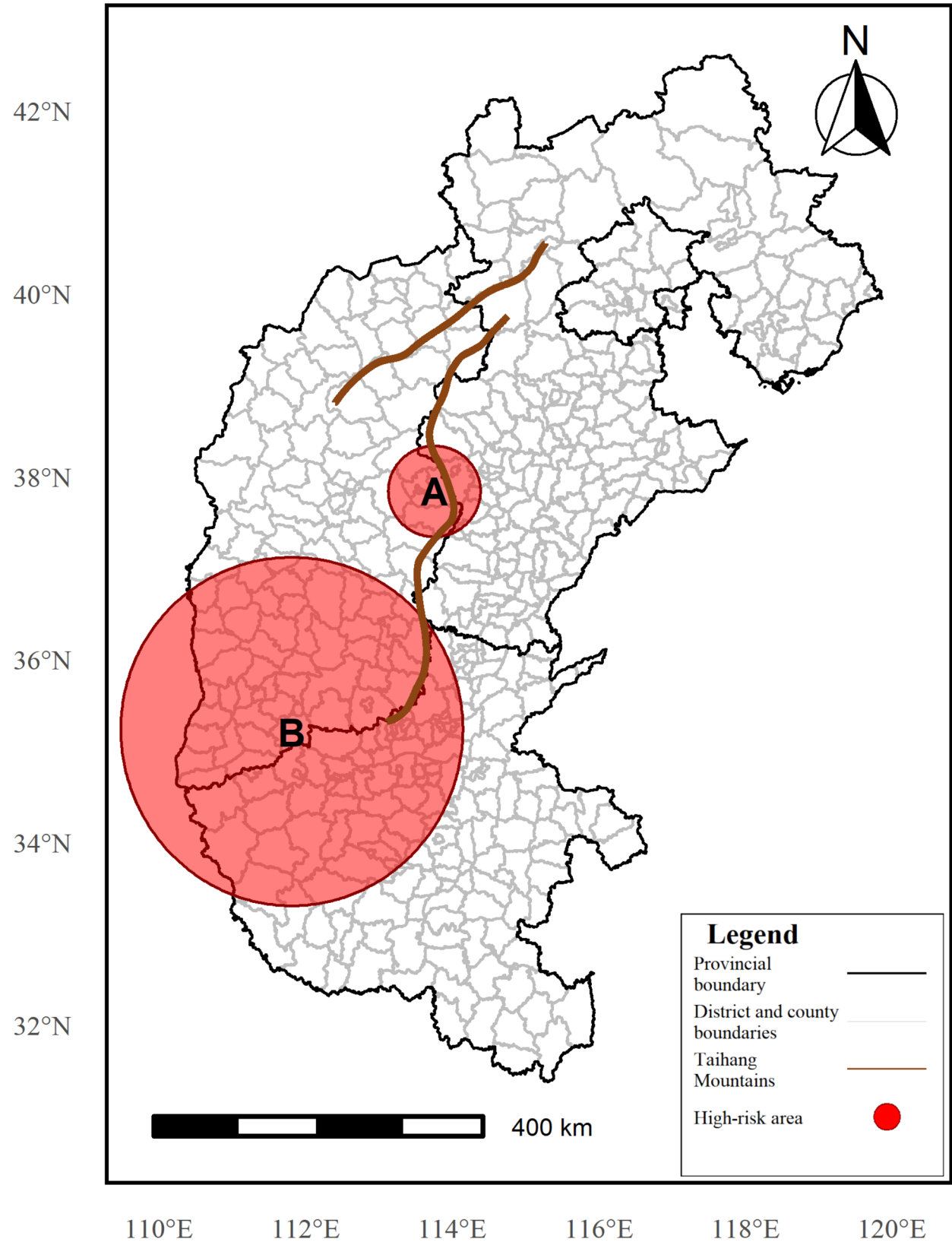


**Fig. 4** The two significant high-risk clusters identified by SaTScan in the study area

**Table 1** High-risk Spatiotemporal clustering of the reported human VL cases from 2006 to 2023

Cluster	Longitude	Latitude	Time window	Number of cases	Relative Risk	The log-likelihood ratio
Cluster A	113.75	37.84	2017–2023	395	239.59	1622.84
Cluster B	111.81	35.21	2020–2023	239	8.10	257.17

**Table 2** Normalized importance of each variable (%IncMSE)

Variables	Normalized importance
Terrain factor†	14.22%
Elevation	14.22%
Environmental factor†	66.17%
Standardized precipitation deviation	17.95%
Forest cumulative change ratio	12.29%
NDVI cumulative change	11.15%
Standardized temperature deviation	9.43%
Urban cumulative change ratio	7.82%
Crop cumulative change ratio	7.54%
Socioeconomic factor†	19.61%
Log of Population	11.00%
GDP	8.61%

**Note:** †Sum of relative contribution for each category.

cases. Elevation exhibits a dual effect: it promotes an increase in cases at elevations below 800 m, but acts as a deterrent beyond this threshold. The cumulative change in forest area ratio and NDVI are positively correlated with the number of cases. Initially, increases in urban cumulative change ratio and GDP suppress the growth of cases, but eventually, they contribute to a rise in case numbers. The cumulative change in cropland ratio also shows a similar nonlinear trend. However, unlike urban cumulative change ratio and GDP, when the horizontal axis is less than 0, it indicates a decrease in cropland. Both cropland reduction and expansion are associated with an increase in VL cases, suggesting that changes in

cropland, regardless of the direction, lead to an increase in the number of cases (Fig. 5).

## Discussion

This study analyzed the spatiotemporal distribution of VL case numbers at the county level in the four major regions surrounding the Taihang Mountains—Beijing, Hebei, Henan, and Shanxi—from 2006 to 2023. A space-time cluster analysis was conducted using SaTScan, which identified two high-risk clusters associated with case aggregation events. The analysis provided the coordinates, time windows, case counts, relative risks, and coverage areas of these clusters. The two time windows began in 2017 and 2020, respectively, and continued until 2023. The persistent high-risk spatiotemporal clustering of VL in the region warrants attention.

Previous studies frequently relied on multi-year averaged variables for modeling, assuming static ecological niches and neglecting the impacts of dynamic changes in driving factors [57, 58]. In contrast, our study incorporated NDVI cumulative change, standardized deviations in temperature and precipitation, and cumulative change in the area proportion of different land cover types into the modeling process. By capturing long-term variations, we highlighted the temporal dynamics of driving factors and emphasized the significant influence of environmental changes on the recurrence and transmission of VL over time. The results from our random forest model further confirm the dominant role of environmental factors, collectively explaining 66.17% of the variation. Notably,

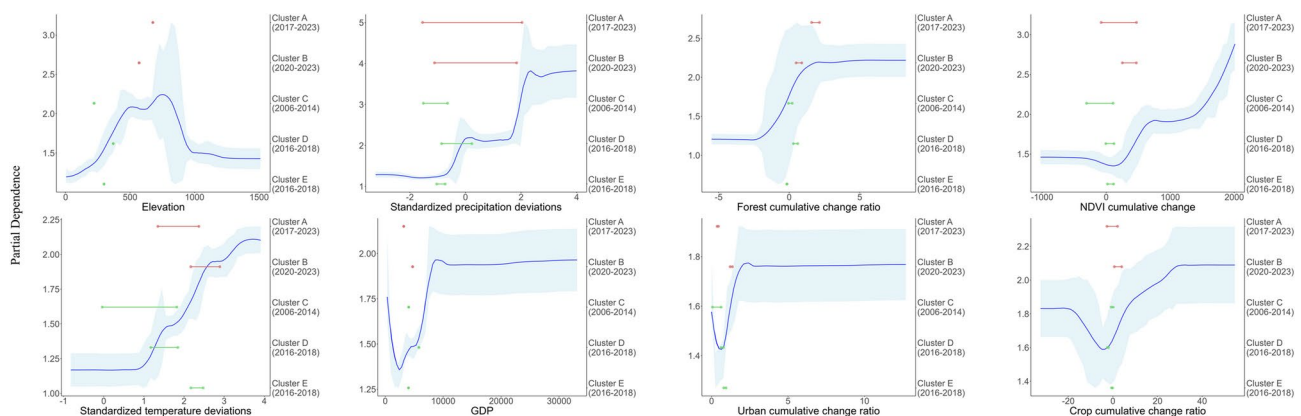


**Fig. 5** The partial dependence plot of each variable. The partial dependence plots isolate the effects of eight feature variables on the predicted number of VL cases. The X-axis represents the range of values for each feature, while the Y-axis shows the model's average predicted value for VL cases. The blue curve represents the average predicted values after 50 iterations, and the shaded area indicates the 95% confidence interval for the predictions over these iterations. The red and green line segments represent the range of feature variable values within different clusters, with red indicating high-risk clusters and green indicating low-risk clusters. These ranges are calculated based on the annual average values of variables across all counties within each cluster



the standardized deviation of precipitation emerged as the most influential variable, followed by elevation, forest cumulative change, and NDVI cumulative change. These findings underscore that long-term environmental changes, including changes in climate factors, NDVI, and land cover, are pivotal in driving the recurrence and transmission of VL in the Taihang Mountain region.

Among these factors, the standardized deviation of precipitation explained 17.95% of the variability in the random forest model, making it the most significant factor influencing VL cases. This factor demonstrated a positive correlation with the number of VL cases. Previous studies have typically used average precipitation and temperature [57, 58], while standardized deviations of precipitation and temperature better capture the long-term trends in precipitation and temperature changes within a region's time series [59]. Additionally, positive precipitation deviations may create more potential habitats for sandflies, the main vectors of VL, thereby increasing the risk of disease transmission [38]. It can be observed that high-risk clusters in the central and western parts of the region exhibit greater standardized precipitation deviations compared to low-risk clusters (Figs. 4 and 5; Figure S1). This distinct difference has influenced the spatial distribution of VL case clusters. The standardized temperature deviations explained 9.43% of the variability. Unlike standardized precipitation deviations, standardized temperature deviations do not significantly influence VL cases when the deviation is less than 1. Only standardized temperature deviations exceeding 1 show a significant positive correlation, suggesting that rapid temperature increases significantly promote disease transmission. Higher temperatures accelerate the metabolic rate of sandflies, shortening their lifecycle from egg laying to adulthood, thereby potentially increasing the rate of VL transmission [36]. In addition, several studies suggested that northern China, including the Taihang Mountain region, would experience significant increases in precipitation [60], and annual mean temperatures are expected to rise by 2.66 °C by mid-century and by 5.62 °C by the end of the 21st century [61]. Thus, the combined effects of increased precipitation and rising temperatures due to climate change may further elevate the risk of VL and expand its endemic areas.

Compared to the previously used NDVI values and land cover type area proportions, we utilized cumulative changes in NDVI and in the area proportion of different land cover types [57, 58]. NDVI cumulative change is positively correlated with VL cases. Its increase often indicates that vegetation is becoming denser, which may provide more favorable habitats and richer food sources for sandflies [50, 62]. Regarding different land cover types area proportion cumulative change, an increase in forest ratio may create ideal breeding grounds for sandflies

[44, 46]. Interestingly, we found that the impact of urban change rate on VL exhibits a U-shaped non-linear pattern in this study. This pattern is consistent with findings from previous research suggesting a link between urban development and VL transmission [63, 64]. Improvements in medical infrastructure, sanitation, and disease control measures associated with urbanization may initially reduce VL transmission risk [53, 65]. However, as urbanization progresses and cities expand into rural or forested areas, human exposure to sandfly habitats may rise, potentially elevating the risk of transmission [66]. In China, land cover changes are primarily driven by policies such as afforestation and urban expansion [67]. In VL endemic areas, integrating land use planning with public health measures is essential for balancing development goals and disease control efforts.

Our study identified elevation as a key factor influencing the transmission of VL, in addition to environmental variables. Elevation accounted for 14.22% of the variation, with a positive correlation observed at altitudes below 800 m. This trend may result from the complex terrain in hilly regions, which provides favorable ecological niches for sandflies [32, 68, 69]. However, at altitudes above 800 m, VL cases declined, likely due to environmental limitations. These findings are consistent with research from high-altitude areas in southern Spain and Henan province, which documented reduced sandfly density and diversity at higher elevations, possibly due to shorter activity periods and less suitable habitats [32, 69, 70]. Nonetheless, isolated reports of sandfly populations thriving above 1,300 m indicate that specific microclimates or adaptive mechanisms may enable their survival [32, 68]. In VL-prone regions, targeted monitoring and control measures should focus on hilly and mountainous areas to address the risk of sandfly-borne transmission.

This study has several limitations. Due to data constraints, our research did not incorporate molecular identification of specific causative parasites (*Leishmania spp.*) or conduct field surveys on sandfly vectors (*Phlebotomus spp.*) and reservoir hosts (e.g., dogs and rodents) [1]. Information on these biological factors is essential for fully understanding the ecological dynamics and transmission mechanisms of visceral leishmaniasis. Therefore, future studies could include molecular analyses of parasites and entomological surveys to enable more precise risk assessment and effective disease control strategies.

## Conclusion

In the past two decades, VL has re-emerged and spread across the regions surrounding the Taihang Mountains, including Beijing, Hebei, Henan, and Shanxi, posing a significant public health challenge. Based on China CDC reports from 2006 to 2023, our study revealed a rapid increase in VL cases in recent years. Long-term

environmental changes, including standardized deviations in temperature and precipitation, cumulative changes in NDVI, and cumulative changes in land cover proportions (such as forest, cropland, and urban areas), have contributed to an increased risk of VL transmission. Additionally, socioeconomic factors, such as population density and GDP, have played a role in the disease's transmission. These findings underscore the importance of integrating environmental monitoring, land use planning, and public health strategies to effectively manage VL risks and protect vulnerable populations.

#### Abbreviations

China CDC	Chinese Center for Disease Control and Prevention
GDP	Gross domestic product
CNY	Chinese Yuan
IGBP	International Geosphere-Biosphere Programme
LLR	Log-likelihood ratio
NDVI	Normalized difference vegetation index
VL	Visceral leishmaniasis

#### Supplementary Information

The online version contains supplementary material available at <https://doi.org/10.1186/s12940-025-01180-9>.

Supplementary Material 1

#### Acknowledgements

The authors would like to thank all participants for participating in this study.

#### Author contributions

FYD and ZM conceived and designed the study. ZM, FYD, PWF and CJZ collected the data and carried out the computations. ZXF, HW, FYD, ZM and TM analyzed the data. ZM, FYD and PWF wrote the paper. SC, HJ, YS, LY, JYY, YPW, MMH, WQX, YQB, QW, KS, XLX, JWZ and DJ gave some useful suggestions to this work. FYD, PWF, TM, HW, and CJZ revised the manuscript. All authors read and approved the final manuscript.

#### Funding

This work was supported by grant from the Tibet University Talent Innovation Team and Laboratory Platform Construction - Plateau Geothermal New Energy Innovation Team and Laboratory Platform Construction (No. 2022ZDTD10), the Base and Talent Program Project of the Xizang Autonomous Region (XZ202501JD0024), the Western Light Project of Chinese Academy of Sciences (No. 17090008), the National Natural Science Foundation of China (No. 42201497), Youth Innovation Promotion Association (No. 2023000117), the Wellcome Trust [Grant number 220211] and Kezhen-Bingwei Young Talent Program.

#### Data availability

The data that support the findings of this study are available on request from the corresponding author.

#### Declarations

##### Ethics approval and consent to participate

Not applicable.

##### Consent for publication

Not applicable.

##### Competing interests

The authors declare no competing interests.

#### Author details

<sup>1</sup>School of Engineering, Tibet University, Lhasa 850000, China

<sup>2</sup>Institute of Geographic Sciences and Natural Resources Research, Chinese Academy of Sciences, Beijing 100101, China

<sup>3</sup>Key Laboratory of Satellite Remote Sensing and Application, Xizang Autonomous Region, Lhasa 850000, China

<sup>4</sup>College of Resources and Environment, University of Chinese Academy of Sciences, Beijing 100049, China

<sup>5</sup>Chinese Center for Disease Control and Prevention (China CDC), Beijing 102206, China

<sup>6</sup>State Key Laboratory of Remote Sensing Science, Aerospace Information Research Institute, Chinese Academy of Sciences, Beijing 100094, China

<sup>7</sup>Nuffield Department of Medicine, Centre for Tropical Medicine and Global Health, University of Oxford, Oxford, UK

<sup>8</sup>Mahidol Oxford Tropical Medicine Research Unit, Faculty of Tropical Medicine, Mahidol University, Bangkok, Thailand

<sup>9</sup>GeoAI Lab, Department of Geography, University at Buffalo, Buffalo, NY, USA

<sup>10</sup>School of Geography & Environmental Science, Guizhou Normal University, Guiyang 550001, China

<sup>11</sup>School of Ecology and Environment, Tibet University, Lhasa 850000, China

<sup>12</sup>Joint Laboratory of Plateau Surface Remote Sensing, Tibet University, Lhasa 850000, China

<sup>13</sup>Yale Institute for Biospheric Studies, Yale University, New Haven, CT, USA

<sup>14</sup>School of the Environment, Yale University, New Haven, CT, USA

Received: 5 February 2025 / Accepted: 19 April 2025

Published online: 04 May 2025

#### References

1. Lun Z-R, Wu M-S, Chen Y-F, Wang J-Y, Zhou X-N, Liao L-F, Chen J-P, Chow LMC, Chang KP. Visceral leishmaniasis in China: an endemic disease under control. *Clin Microbiol Rev.* 2015;28(4):987–1004.
2. Desjeux P. Leishmaniasis: current situation and new perspectives. *Comp Immunol Microbiol Infect Dis.* 2004;27(5):305–18.
3. Ghazanfar M, Malik MF. Sandfly and leishmaniasis: A review. *J Ecosyst Ecography* 2016, 6(3).
4. Scarpini S, Dondi A, Totaro C, Biagi C, Melchionda F, Zama D, Pierantoni L, Gennari M, Campagna C, Prete A et al. Visceral leishmaniasis: epidemiology, diagnosis, and treatment regimens in different geographical areas with a focus on pediatrics. *Microorganisms* 2022, 10(10).
5. Karimi A, Alborzi A, Amanati A. Visceral leishmaniasis: an update and literature review. *Archives Pediatr Infect Dis* 2016, 4(3).
6. Faleiro RJ, Kumar R, Hafner LM, Engwerda CR. Immune regulation during chronic visceral leishmaniasis. *PLoS Negl Trop Dis.* 2014;8(7):e2914.
7. Murray HW, Berman JD, Davies CR, Saravia NG. Advances in leishmaniasis. *Lancet.* 2005;366(9496):1561–77.
8. Sakkas H, Gartzonika C, Levidiotou S. Laboratory diagnosis of human visceral leishmaniasis. *J Vector Borne Dis* 2016, 53(1).
9. Organization WH. Control of the leishmaniases. World Health Organization technical report series 2010(949):xii.
10. Burki T. East African countries struggle with visceral leishmaniasis. *Lancet.* 2009;374(9687):371–2.
11. Torres-Guerrero E, Quintanilla-Cedillo MR, Ruiz-Esmenjaud J, Arenas R. Leishmaniasis: a review. *F1000Res.* 2017, 6:750.
12. Guan L-R, Wu Z-X. Historical experience in the elimination of visceral leishmaniasis in the plain region of Eastern and central China. *Infect Dis Poverty.* 2014;3:1–12.
13. Chung H-L. A resume of kala-azar work in China. *Chin Med J.* 1953;71(06):421–64.
14. Zhi-Biao X. Present situation of visceral leishmaniasis in China. *Parasitol Today.* 1989;5(7):224–8.
15. Bassett-Smith PW. Kala-Azar in the Far East. *Br Med J.* 1909;2(2553):1614.
16. Cochran S. Distribution of Kala-Azar in China and Korea. A reprint. *Chin Med J.* 1914;28(04):274–6.
17. Wang Z, Xiong G, Guan L. Epidemiology and prevention of kala-azar in China. *Zhonghua Liu Xing Bing Xue Za zhi = Zhonghua Liuxingbingxue Zazhi.* 2000;21(1):51–4.

18. Li-Ren G, Wei-Xia S. Recent advances in visceral leishmaniasis in China. *South-east Asian J Trop Med Public Health*. 1991;22:291.
19. WANG C-T, WU C-C. Studies on kala-azar in new China. *Chin Med J*. 1959;78(01):55–71.
20. Li Y, Zhong W, Zhao G, Wang H. Prevalence and control of kala-azar in China. *J Pathog Biol*. 2011;6:629–31.
21. Ding F, Wang Q, Fu J, Chen S, Hao M, Ma T, Zheng C, Jiang D. Risk factors and predicted distribution of visceral leishmaniasis in the Xinjiang Uygur autonomous region, China, 2005–2015. *Parasit Vectors*. 2019;12(1):528.
22. HAN S, WU W-p XUE, C-z DINGW, HOU Y-y FENG Y, ZHONG B, CAO L et al. ZHANG Y-n, JIANG X-f: Endemic status of visceral leishmaniasis in China from 2004 to 2016. *Chinese Journal of Parasitology and Parasitic Diseases*. 2019, 37(2):7.
23. Zheng C, Wang L, Li Y, Zhou XN. Visceral leishmaniasis in Northwest China from 2004 to 2018: a spatio-temporal analysis. *Infect Dis Poverty*. 2020;9(1):165.
24. Zhao Y, Jiang D, Ding F, Hao M, Wang Q, Chen S, Xie X, Zheng C, Ma T. Recurrence and Driving Factors of Visceral Leishmaniasis in Central China. *Int J Environ Res Public Health*. 2021, 18(18).
25. Muñoz-Sabater J, Dutra E, Agustí-Panareda A, Albergel C, Arduini G, Balsamo G, Boussetta S, Choulga M, Harrigan S, Hersbach H. ERA5-Land: A state-of-the-art global reanalysis dataset for land applications. *Earth Syst Sci Data*. 2021;13(9):4349–83.
26. Yearbook CS. China statistical yearbook. Beijing: Zhongguo tongji chubanshe, various years 2024.
27. Guo R, Guo R. Hebei. Regional China: A Business and Economic Handbook. 2013:108–117.
28. Silva CRd, Wang H, Zhu Y, Wang J, Han H, Niu J, Chen X. Modeling of Spatial pattern and influencing factors of cultivated land quality in Henan Province based on Spatial big data. *PLoS ONE* 2022, 17(4).
29. Zhang H, Yang Y. Analysis on the Contribution of Industrial Structure Optimization to Regional Economic Growth in Shanxi Province. In: 2021 International Conference on Diversified Education and Social Development (DESD 2021): 2021: Atlantis Press; 2021:236–243.
30. Guan L. A supplement to the research on sandfly biology in China. *Int J Med Parasit Dis*. 2010;37(2):65–7.
31. Ballart C, Baron S, Alcover MM, Portus M, Gallego M. Distribution of phlebotomine sand flies (Diptera: Psychodidae) in Andorra: first finding of *P. perniciosus* and wide distribution of *P. ariasi*. *Acta Trop*. 2012;122(1):155–9.
32. Diaz-Saez V, Corpas-Lopez V, Merino-Espinosa G, Morillas-Mancilla MJ, Abat-touy N, Martin-Sanchez J. Seasonal dynamics of phlebotomine sand flies and autochthonous transmission of leishmania infantum in high-altitude ecosystems in Southern Spain. *Acta Trop*. 2021;213:105749.
33. Reuter HI, Nelson A, Jarvis A. An evaluation of void-filling interpolation methods for SRTM data. *Int J Geogr Inf Sci*. 2007;21(9):983–1008.
34. Leal Filho W, Nagy GJ, Gbaguidi GJ, Paz S, Dinis MAP, Luetz JM, Sharifi A. The role of Climatic changes in the emergence and re-emergence of infectious diseases: bibliometric analysis and literature-supported studies on zoonoses. *One Health Outlook*. 2025;7(1):12.
35. Abdullahi B, Mutiso J, Maloba F, Macharia J, Riongoita M, Gicheru M, Chowdhury R. Climate change and environmental influence on prevalence of visceral leishmaniasis in West Pokot County, Kenya. *J Trop Med*. 2022;2022:1–6.
36. Benkova I, Volf P. Effect of temperature on metabolism of phlebotomus Papatasi (Diptera: Psychodidae). *J Med Entomol*. 2007;44(1):150–4.
37. Hamta A, Saghaipour A, Zanjirani Farahani L, Moradi Asl E, Ghorbani E. The Granger causality analysis of the impact of Climatic factors on visceral leishmaniasis in Northwestern Iran in 1995–2019. *J Parasit Dis*. 2021;45(1):17–23.
38. Vieira VR, de Aguiar GM, de Azevedo ACR, Rangel EF, Guimaraes AE. Sand fly population dynamics in areas of American cutaneous leishmaniasis, municipality of Paraty, Rio de Janeiro, Brazil. *Sci Rep*. 2023;13(1):3622.
39. Vivero RJ, Torres-Gutierrez C, Bejarano EE, Pena HC, Estrada LG, Florez F, Ortega E, Aparicio Y, Muskus CE. Study on natural breeding sites of sand flies (Diptera: Phlebotominae) in areas of leishmania transmission in Colombia. *Parasit Vectors*. 2015;8:116.
40. Hong XG, Zhu Y, Wang T, Chen JJ, Tang F, Jiang RR, Ma XF, Xu Q, Li H, Wang LP, et al. Mapping the distribution of sandflies and sandfly-associated pathogens in China. *PLoS Negl Trop Dis*. 2024;18(7):e0012291.
41. Ge Q, Hao M, Ding F, Jiang D, Scheffran J, Helman D, Ide T. Modelling armed conflict risk under climate change with machine learning and time-series data. *Nat Commun*. 2022;13(1):2839.
42. Kotz M, Levermann A, Wenz L. The effect of rainfall changes on economic production. *Nature*. 2022;601(7892):223–7.
43. Figueiredo ABF, Werneck GL, Cruz MdSp, Silva Jpd A, ASd. Land use, land cover, and prevalence of canine visceral leishmaniasis in Teresina, Piauí State, Brazil: an approach using orbital remote sensing. *Cadernos De Saúde Pública* 2017, 33(10).
44. Hage RDS, Nunes ESSV, Bohm BC, Lima JV, Bruhn NCP, Menezes GR, Bruhn FRP. Spatiotemporal relationship between agriculture, livestock, deforestation, and visceral leishmaniasis in Brazilian legal Amazon. *Sci Rep*. 2024;14(1):21542.
45. de Souza WM, Weaver SC. Effects of climate change and human activities on vector-borne diseases. *Nat Rev Microbiol*. 2024;22(8):476–91.
46. Jagadeesh S, Combe M, Ginouves M, Simon S, Prevot G, Couppie P, Nacher M, Gozlan RE. Spatial variations in leishmaniasis: A biogeographic approach to mapping the distribution of leishmania species. *One Health*. 2021;13:100307.
47. Pinto Moraes JL, Marinho Santana HT, Conceição Abreu Bandeira M, Macário Rebêlo JM. Effects of forest degradation on the sand fly communities of Northeast Brazil. *J Vector Ecol*. 2020;45(1):89–99.
48. Sulla-Menashe D, Friedl MA. User guide to collection 6 MODIS land cover (MCD12Q1 and MCD12C1) product. 2018.
49. Tri W, Ivo E, Supalert N, Rawadee K, Soawapak H, Kittipong C, Nicholas D, Serge M. The estimated burden of scrub typhus in Thailand from National surveillance data (2003–2018). *PLoS Negl Trop Dis*. 2020;14:e0008233.
50. Chanampa MDM, Gleiser RM, Hoyos CL, Copa GN, Mangudo C, Nasser JR, Gil JF. Vegetation cover and microspatial distribution of sand flies (Diptera: Psychodidae) in an endemic locality for cutaneous leishmaniasis in Northern Argentina. *J Med Entomol*. 2018;55(6):1431–9.
51. Didan K, Munoz AB, Solano R, Huete A. MODIS vegetation index user's guide (MOD13 series). Univ Arizona: Veg Index Phenology Lab. 2015;35:2–33.
52. Parham PE, Waldock J, Christophides GK, Hemming D, Augusto F, Evans KJ, Fefferman N, Gaff H, Gumel A, LaDeau S et al. Climate, environmental and socio-economic change: weighing up the balance in vector-borne disease transmission. *Philos Trans R Soc Lond B Biol Sci*. 2015, 370(1665).
53. Organization WH. Vector-borne diseases. In: WHO Regional Office for South-East Asia; 2014.
54. Grifferty G, Shirley H, McGloin J, Kahn J, Orriols A, Wamai R. Vulnerabilities to and the socioeconomic and psychosocial impacts of the leishmaniasis: A review. *Res Rep Trop Med*. 2021;12:135–51.
55. José Cláudio S, Cassiano V, Carlos Magno Castelo Branco F. Factors affecting the Spatial distribution of visceral leishmaniasis in an urban area of recent emergence in inner Brazil. *Int J Trop Dis* 2021, 4(2).
56. Chen J, Gao M, Cheng S, Hou W, Song M, Liu X, Liu Y. Global 1 Km x 1 Km grid-based revised real gross domestic product and electricity consumption during 1992–2019 based on calibrated nighttime light data. *Sci Data*. 2022;9(1):202.
57. Hao Y, Luo Z, Zhao J, Gong Y, Li Y, Zhu Z, Tian T, Wang Q, Zhang Y, Zhou Z et al. Transmission risk prediction and evaluation of Mountain-Type zoonotic visceral leishmaniasis in China based on Climatic and environmental variables. *Atmosphere* 2022, 13(6).
58. Wu X, Wen X, Song S, Zhao C, Shao Z, Liu K, Fu T. Global distribution and prediction of Transmission-Risk of visceral leishmaniasis. *Zoonoses* 2024, 4(1).
59. Robinson A, Lehmann J, Barriopedro D, Rahmstorf S, Coumou D. Increasing heat and rainfall extremes now far outside the historical climate. *Npj Clim Atmospheric Sci* 2021, 4(1).
60. Tian J, Zhang Z, Ahmed Z, Zhang L, Su B, Tao H, Jiang T. Projections of precipitation over China based on CMIP6 models. *Stoch Env Res Risk Assess*. 2021;35(4):831–48.
61. You Q, Cai Z, Wu F, Jiang Z, Pepin N, Shen SS. Temperature dataset of CMIP6 models over China: evaluation, trend and uncertainty. *Clim Dyn*. 2021;57:17–35.
62. Poché DM, Poché RM, Mukherjee S, Frankowiak GA, Briley LN, Somers DJ, Garlapati RB. Phlebotomine sandfly ecology on the Indian Subcontinent: does village vegetation play a role in sandfly distribution in Bihar, India? *Med Vet Entomol*. 2017;31(2):207–13.
63. Reis LLD, Balieiro A, Fonseca FR, Gonçalves MJF. Changes in the epidemiology of visceral leishmaniasis in Brazil from 2001 to 2014. *Rev Soc Bras Med Trop*. 2017;50(5):638–45.
64. Cavalcante FRA, Cavalcante KKS, Florencio C, Moreno JO, Correia FGS, Alencar CH. Human visceral leishmaniasis: epidemiological, Temporal and spacial aspects in Northeast Brazil, 2003–2017. *Rev Inst Med Trop Sao Paulo*. 2020;62:e12.
65. da Silva Santana Cruz C, Soeiro Barbosa D, Oliveira VC, Cardoso DT, Guimaraes NS, Carneiro M. Factors associated with human visceral leishmaniasis cases during urban epidemics in Brazil: a systematic review. *Parasitology*. 2021;148(6):639–47.

66. Ursine RL, Rocha MF, Sousa JFd S, RCd, Soares MD, Gusmão MSF, Leite ME, Vieira TM. American tegumentary leishmaniasis in an endemic municipality in the North of Minas Gerais State: Spatial analysis and socio-environmental factors. *Revista Do Instituto De Medicina Tropical De São Paulo* 2021, 63.
67. Kuang W. National urban land-use/cover change since the beginning of the 21st century and its policy implications in China. *Land Use Policy* 2020, 97.
68. Gomez EA, Kato H, Mimori T, Hashiguchi Y. Distribution of *Lutzomyia aya-cuchensis*, the vector of Andean-type cutaneous leishmaniasis, at different altitudes on the Andean slope of Ecuador. *Acta Trop.* 2014;137:118–22.
69. He Z, Wang D, Kou Y, Yang C, Sun Y, Ji P, Jiang T, Lu D, Qian D, Zhang H, et al. Distribution and seasonal fluctuation of visceral leishmaniasis vectors sandflies in Henan Province in 2023. *Zhongguo Xue Xi Chong Bing Fang Zhi Za Zhi.* 2024;36(4):346–51.
70. Ballart C, Guerrero I, Castells X, Barón S, Castillejo S, Alcover MM, Portús M, Gállego M. Importance of individual analysis of environmental and Climatic factors affecting the density of leishmania vectors living in the same geographical area: the example of *phlebotomus Ariasi* and *P. perniciosus* in Northeast Spain. *Geospat Health.* 2014;8(2):389–403.

### Publisher's note

Springer Nature remains neutral with regard to jurisdictional claims in published maps and institutional affiliations.